ARTICLES

Functional Attenuation of Ufd1l, a 22q11.2 Deletion Syndrome Candidate Gene, Leads to Cardiac Outflow Septation Defects in Chicken Embryos

CHIHIRO YAMAGISHI, BEEREND P. HIERCK, ADRIANA C. GITTENBERGER-DE GROOT,
HIROYUKI YAMAGISHI, AND DEEPAK SRIVASTAVA

*Departments of Pediatrics and Molecular Biology [C.Y., H.Y., D.S.], University of Texas Southwestern
Medical Center at Dallas, Dallas, TX, 75390-9148, U.S.A.; and Department of Anatomy and Embryology
[B.P.H., A.C.G.], Leiden University Medical Center, Leiden, Netherlands*

ABSTRACT

Microdeletion of chromosome 22q11.2 is commonly associated with congenital cardiovascular defects that involve development of cranial neural crest cells (NCC) that emigrate through the pharyngeal arches. *UFD1l* is one of several candidate genes for 22q11.2 deletion syndrome (22q11DS). *UFD1l* encodes a protein whose yeast counterpart is involved in a ubiquitin-dependent proteolytic degradation pathway; however, the role of UFD1L in NCC development remains unknown. Mouse embryos that lack *Ufd1l* die before organogenesis. We have therefore studied the function of Ufd1l in the chick system. Chick *Ufd1l* encoded a 307–amino acid protein that was highly conserved with mouse and human UFD1L. Chick Ufd1l was expressed in the developing neural tube, NCC, and mesenchyme of the head and pharyngeal arch structures, as well as in the conotruncal region (cardiac outflow tract), consistent with the clinical features of 22q11DS. To determine loss-of-function effects of chick Ufd1l in NCC, we infected cardiac NCC with a retrovirus expressing antisense Ufd1l transcripts in chick embryos before their migration. Morphologic analysis of infected embryos at a later developmental stage demonstrated that functional attenuation of chick Ufd1l in cardiac NCC resulted in an increased incidence of conotruncal septation defects. These data suggest that Ufd1l may play a role in cardiac NCC during conotruncal septation. (*Pediatr Res* **53:** 546–553, 2003)

Abbreviations
CVD, cardiovascular defects
del.22q11, microdeletion of chromosome 22q11.2
ET$_A$, endothelin receptor A
HH, Hamburger and Hamilton
NCC, neural crest cells
VSD, ventricular septal defect
22q11DS, 22q11.2 deletion syndrome

Monoallelic microdeletion of chromosome 22q11.2 (del.22q11) is the most common human chromosomal deletion and results in the 22q11.2 deletion syndrome (22q11DS), with an estimated frequency of 1 in 4000–5000 births (1). 22q11DS encompasses three independently established syndromes, including DiGeorge syndrome, velo-cardio-facial syndrome, and conotruncal anomaly face syndrome, and manifests a variety of features, including craniofacial and cardiovascular defects (CVD) and behavioral and psychiatric disorders (2–4). 22q11DS is associated with specific types of CVD that are characterized as malformations of the conotruncus (outflow tract of the heart) or the aortic arch, including persistent truncus arteriosus, tetralogy of Fallot, and interrupted aortic arch, type B (5). The craniofacial defects and CVD in 22q11DS result from defects of embryonic structures populated by migrating cranial and cardiac neural crest cells (NCC) that originate from the caudal hindbrain (6, 7). Ablation of cardiac NCC in chick embryos results in persistent truncus arteriosus, aortic arch malformations, and hypoplasia of thymus and parathyroid glands similar to that observed in patients with 22q11DS (6, 7). This suggests that studies on candidate genes in the 22q11.2

region that are involved in the development of cardiac NCC may provide insight into the molecular mechanisms underlying the 22q11DS and its associated CVD.

More than 90% of patients with 22q11DS have a similar del.22q11, commonly spanning 1.5–3 megabases in size (8). More than 30 genes have been identified in the deleted region. Recent studies show that haploinsufficiency of *Tbx1*, one of the genes in this region, is likely to be the major determinant of aortic arch defects in patients with 22q11DS (9–11). However, no single gene mutation, including that of *TBX1*, that results in the 22q11DS phenotype has yet been detected (12, 13). Our screen for mouse genes dependent on dHAND, a transcription factor implicated in NCC development, previously identified *Ufd1l*, whose human ortholog had been mapped to 22q11.2 (14, 15). *UFD1L* encodes a highly conserved protein from yeast to human that is involved in the degradation of ubiquitinated proteins. Mouse *Ufd1l* was expressed in many embryonic tissues affected in patients with 22q11DS, including the pharyngeal arches, palatal precursors, the frontonasal region, telencephalon, and the cardiac outflow tract. Human *UFD1L* was deleted in >180 patients studied with 22q11DS (15). A smaller deletion of exon 1 to 3 of *UFD1L* and its neighboring gene, *CDC45*, which encodes a putative cell cycle regulating protein, was found in one individual with the phenotype of 22q11DS. These results suggest that *UFD1L* may be implicated in some features of 22q11DS, although the very early lethality of mice that lack *Ufd1l* precludes an understanding of the role of UFD1L in cardiac NCC development (16).

The avian system is well established to study NCC development, as gene constructs can be specifically introduced into the chick NCC lineage using a replication-incompetent retrovirus system (17). To take advantage of the avian system, we cloned the chick ortholog of *UFD1L* and performed expression and functional analyses of chick Ufd1l during embryogenesis, focusing on cardiac NCC development. Chick *Ufd1l* was expressed in a variety of developing tissues with enhanced expression in the cardiac outflow tract and neural crest-derived mesenchyme of pharyngeal arches and aortic arch arteries, similar to mouse *Ufd1l*. Attenuation of chick Ufd1l expression in premigratory cardiac NCC resulted in an increased number of conotruncal septation defects. These data suggest that Ufd1l may play a role in the development of cardiac NCC that contribute to conotruncal septation.

METHODS

Cloning of chick Ufd1l. A stage 12–15 chick embryo library in lambdaZAPII was screened according to the manufacturer's instructions (Stratagene), with chick Ufd1l partial cDNA (741bp) that was obtained from Hamburger and Hamilton (HH) stage 12 chick total RNA by reverse-transcribed PCR. Approximately 1 μg of total RNA was reverse transcribed using M-MuLV transcriptase (Roche). One microliter of the first-strand cDNA produced was used as template for PCR reactions using specific oligonucleotide amplimers (5'-GGAGAAAGGAGGGAAGATAA-3', 5'-GCTTCATCCTCT-TCAACCTT-3') derived from mouse Ufd1l cDNA. 5' rapid amplification of cDNA ends was then performed to obtain full-length cDNA according to manufacture's instructions (Clontech).

Northern analysis. Total RNA from several chick tissues at embryonic day 18 was electrophoresed, transferred to a nylon membrane, and hybridized with a ^{32}P-labeled full-length chick Ufd1l cDNA probe. Hybridization was performed in Rapid-hyb buffer (Amersham) at 65°C overnight and washed with 2 × salt-sodium chloride/0.1% SDS at room temperature for 10 min and 1x salt-sodium phosphate-EDTA/1% SDS at 65°C for 15 min. Nylon membrane was exposed to x-ray film (Kodak).

Collection of chick embryos and primary NCC culture experiments. Fertilized eggs were incubated at 37°C to obtain chick embryos of HH stage 10–26. The cranial neural fold from the otic vesicle to somite 3 of stage 9–11 chick embryos was dissected and treated with 0.5 mg/mL collagenase type II in PBS at 37°C for 2–3 min to remove the mesenchyme surrounding the neural tube. The isolated neural tube was washed in Dulbecco's modified Eagle's medium including 10% fetal bovine serum, then placed on gelatin-coated culture plates. The dissected neural tubes were cultured at 37°C for 36–48 h in Dulbecco's modified Eagle's medium including 10% fetal bovine serum to allow NCC to migrate from the neural tubes onto culture plates. NCC were fixed with 4% paraformaldehyde/PBS. *In situ* hybridization and immunohistochemistry were subsequently performed. All experimental procedures were performed according to the current local guidelines for animal experiments in the University of Texas Southwestern Medical Center and Leiden University Medical Center.

RNA in situ hybridization. RNA *in situ* hybridization of chick embryos and cultured NCC was performed as previously described (18) with digoxigenin-labeled Ufd1l riboprobes synthesized from a 741-bp fragment of chick Ufd1l cDNA. Briefly, chick embryos of varying stages were isolated, and the pericardium was removed. Embryos were fixed in 4% paraformaldehyde/PBS at 4°C overnight. Embryos were treated with proteinase K (30 μg/mL) for 3–20 min at room temperature depending on their stage of development. Prehybridization was performed at 61°C for 3 h in solution containing 50% formamide, 4× salt-sodium chloride, 1× Denhardt's solution, 500 μg/mL salmon sperm DNA, 250 μg/mL yeast tRNA, and 10% dextran sulfate. Hybridization was performed in the same solution for 18 h. After a series of washes, embryos were treated in 2% blocking solution for 2 h and incubated with antidigoxigenin antibody for 1 h at room temperature. Color reaction was performed at room temperature in substrate color reaction mixture for 12–18 h and terminated by fixing embryos in 4% paraformaldehyde/0.1% glutaraldehyde.

Radioactive *in situ* hybridization was performed using ^{35}S-labeled antisense riboprobes synthesized with T7 or SP6 RNA polymerase (MAXIscript, Ambion Inc.) from chicken dHAND or neuropilin-1 full-length cDNA, respectively. Paraffin-embedded coronal sections of HH stage 18 control embryos and antisense Ufd1l-infected embryos were hybridized with probes as previously described (18). Plasmids for dHAND and neuropilin-1 riboprobe are available upon request.

Fixed NCC were treated with proteinase K (30 μg/mL) for 5 min at 37°C. After postfixation with 4% paraformaldehyde/

PBS, cells were dehydrated in methanol. *In situ* hybridization was performed at 61°C for 18 h as described above.

Immunocytochemistry. For immunocytochemistry, fixed and dehydrated NCC were incubated with 3% H_2O_2 for 30 min at room temperature. After rehydration, cells were incubated in blocking solution [3% BSA, 0.1% Igepal (Sigma Chemical Co.) in PBS] at room temperature for 30 min and then incubated in primary antibody, anti–HNK-1/N-CAM (Sigma Chemical Co.; 1:60), at room temperature for 60 min. After several washes in PBS, conjugated secondary antibody [anti-mouse IgM (1:50)] was applied to the cells and incubated at room temperature for 60 min. The cells were then incubated in developing solution [0.03% 3-3'-diaminobenzidine tetrahydrochloride (Sigma Chemical Co.) -0.1% TritonX in PBS] at room temperature for 10 min. Color reaction was performed in 0.03% H_2O_2 at room temperature for 10 min. After several washes in PBS, cells were fixed with 4% paraformaldehyde/0.1% glutaraldehyde for 12–24 h.

In vitro transcription and translation. The full-length chick Ufd1l cDNA was cloned in the sense and antisense direction into pBluescript plasmids. Mouse endothelin receptor A (ET_A) was also cloned in antisense direction into pBluescript plasmids as a control. All plasmids were linearized with *Sma*I for *in vitro* transcription and translation reactions using TNT-coupled Reticulocyte Lysate System (Promega) with T7 RNA polymerase. One microgram of sense cUfd1l plasmid and antisense cUfd1l or ET_A plasmid were mixed together in the same tube for transcription and translation. A sense cUfd1l plasmid and pBluescript plasmid mixture was performed simultaneously as a control. Translated products were labeled with [^{35}S] methionine (Amersham) and determined by SDS-PAGE and autoradiography. The signals were quantified using ImageQuant software (Molecular Dynamics).

Retrovirus infection of chick embryos. The full-length chick Ufd1l cDNA was cloned in the sense and antisense direction into the proretroviral pCXIZ vector (gift from Dr. Takashi Mikawa). All retroviral constructs were stably transfected to the D17.2G helper cell line for virus production. *In vivo* infection of premigrating NCC in chick embryos was performed at HH stage 9–11 as described previously (19, 20). The embryos were allowed to develop in ovo until HH stage 31–32 and then were harvested and fixed with 4% paraformaldehyde for histologic analysis. HH stage 18 embryos were also harvested for section *in situ* hybridization using dHAND and neuropilin-1 riboprobes.

In vitro infection was performed on neural tube dissected from HH stage 9–11 as described above. After NCC migration, β-galactosidase activity was detected by using X-gal as described previously (21).

Histology. Embryos were embedded in paraffin, and serial transverse sections were obtained. The transverse sections of embryos after retrovirus infection or control embryos were stained with hematoxylin and eosin.

RESULTS

Chick Ufd1l *cDNA.* The largest cDNA obtained of chick *Ufd1l* by library screening followed by 5' rapid amplification of

cDNA ends contained 1026 nucleotides. Chick *Ufd1l* was predicted to encode a 307–amino acid protein and was highly conserved with its murine (94% identical, 96% similar) and human (94% identical, 96% similar) counterparts (Fig. 1A). Although the previously cloned human UFD1L protein (as translated from cDNA, GenBank accession number U64444) (14) showed a tandem repetition of a 36–amino acid domain that was present in the yeast, chicken, and mouse as a single copy, the protein sequences predicted from all human UFD1L cDNAs that we cloned (GenBank accession number
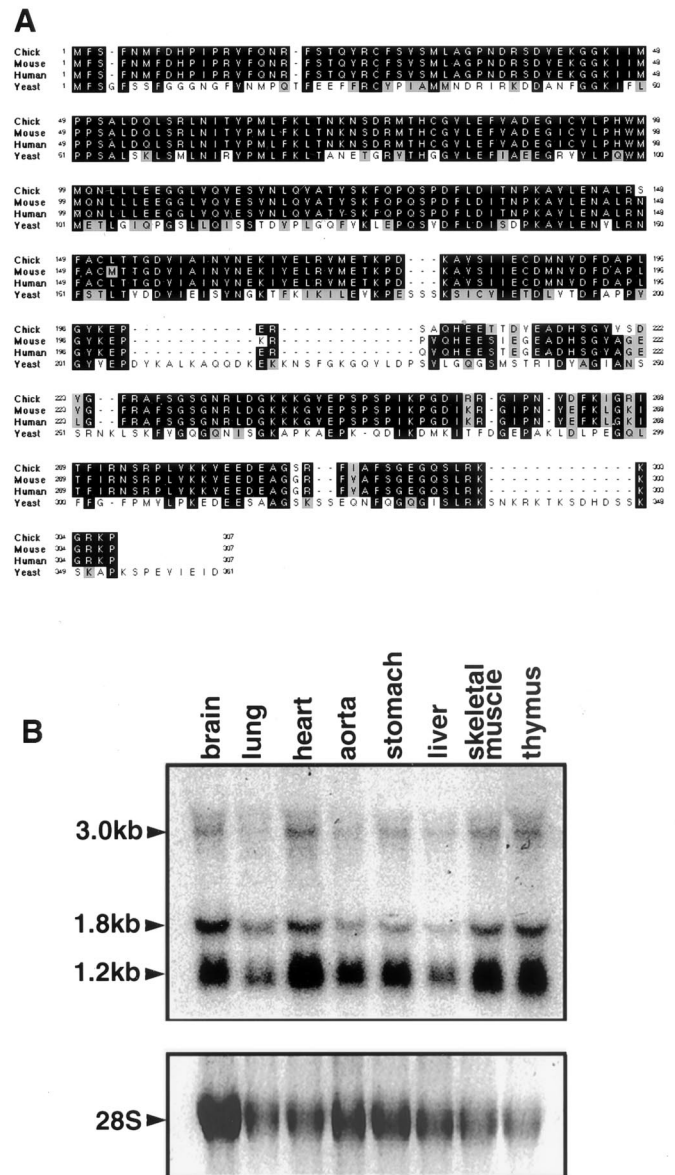

Figure 1. Sequence and expression of chick Ufd1l. *A*, Sequence alignment of full-length chick Ufd1l with mouse, human, and yeast Ufd1l. Amino acid residues that are identical or similar are shaded in black or gray, respectively. Chick *Ufd1l* encodes a 307–amino acid protein and is highly conserved with its murine (94% identical, 96% similar) and human (94% identical, 96% similar) counterparts. It was 36% identical and 50% similar to yeast Ufd1. *B*, Northern blot analysis of chick Ufd1l in embryonic day 18 tissues. mRNA transcripts (1.2, 1.8, and 3.0 kb) were present in all tissues examined. The expression levels of chick Ufd1l in brain, heart, skeletal muscle, and thymus were higher than in other tissues.

AY101594) did not contain such a domain and were more similar to those of other species. Chick Ufd1l was also 36% identical and 50% similar to yeast Ufd1. Nucleotide and protein sequences of chick Ufd1l are available at NCBI (GenBank accession number AF407671).

Expression pattern of chick Ufd1l. Northern blot analysis of total RNA from several chick tissues at embryonic day 18 was performed using full-length chick Ufd1l cDNA as a probe. mRNA transcripts (1.2, 1.8, and 3.0 kb) were present in all tissues examined and possibly represented alternatively spliced forms (Fig. 1B). The expression level of chick Ufd1l in each tissue was variable, with expression in brain, heart, skeletal muscle, and thymus relatively higher than in other tissues.

To determine the expression pattern of chick *Ufd1l* during embryogenesis, *in situ* hybridization analysis was performed. Chick *Ufd1l* was detectable by stage 7 in the neural plate (data not shown). At stage 10, as the neural tube and somites formed, expression throughout the neural tube was apparent (Fig. 2A). At later stages, chick *Ufd1l* was expressed in many tissues, with marked expression in the head, pharyngeal arches, frontonasal region, neural tube, and limb buds (Fig. 2, B and C). Whole-mount *in situ* hybridization on the heart dissected from embryos at stage 26, when conotruncal septation takes place, demonstrated strong expression of chick *Ufd1l* in the conotruncal region of the heart and in emerging aortic arch arteries (Fig.

2D). The expression of chick *Ufd1l* in the neural tube and mesenchymal cells along the pharyngeal arch arteries was detected in transverse sections through chick embryos after whole-mount *in situ* hybridization (Fig. 2, E and F). The overall embryonic expression pattern of chick *Ufd1l* was similar to that of mouse (14, 15) and consistent with some of the clinical features of 22q11DS.

To determine whether chick Ufd1l was expressed in migrating NCC, we examined primary chick NCC cultures. NCC that had migrated off chick neural tube in culture exhibited normal expression of the avian NCC marker HNK-1 by immunocytochemistry (Fig. 3A). *In situ* hybridization in the cultured NCC demonstrated chick Ufd1l expression in the migrating NCC, consistent with the result of whole-mount *in situ* hybridization analysis on embryos (Fig. 3, B and C).

Functional attenuation of chick Ufd1l by retroviral infection. To investigate the functional role of chick Ufd1l in cardiac NCC, we used a well-established gene introduction system in chick NCC using a replication-incompetent retrovirus (17). To study loss of function effects *in vivo*, we prepared a Ufd1l antisense retroviral vector that would generate Ufd1l antisense transcripts. To determine first whether the Ufd1l antisense transcripts might interfere with normal translation of Ufd1l sense transcripts, we performed *in vitro* transcription and translation experiments. As shown in Figure 4, the protein
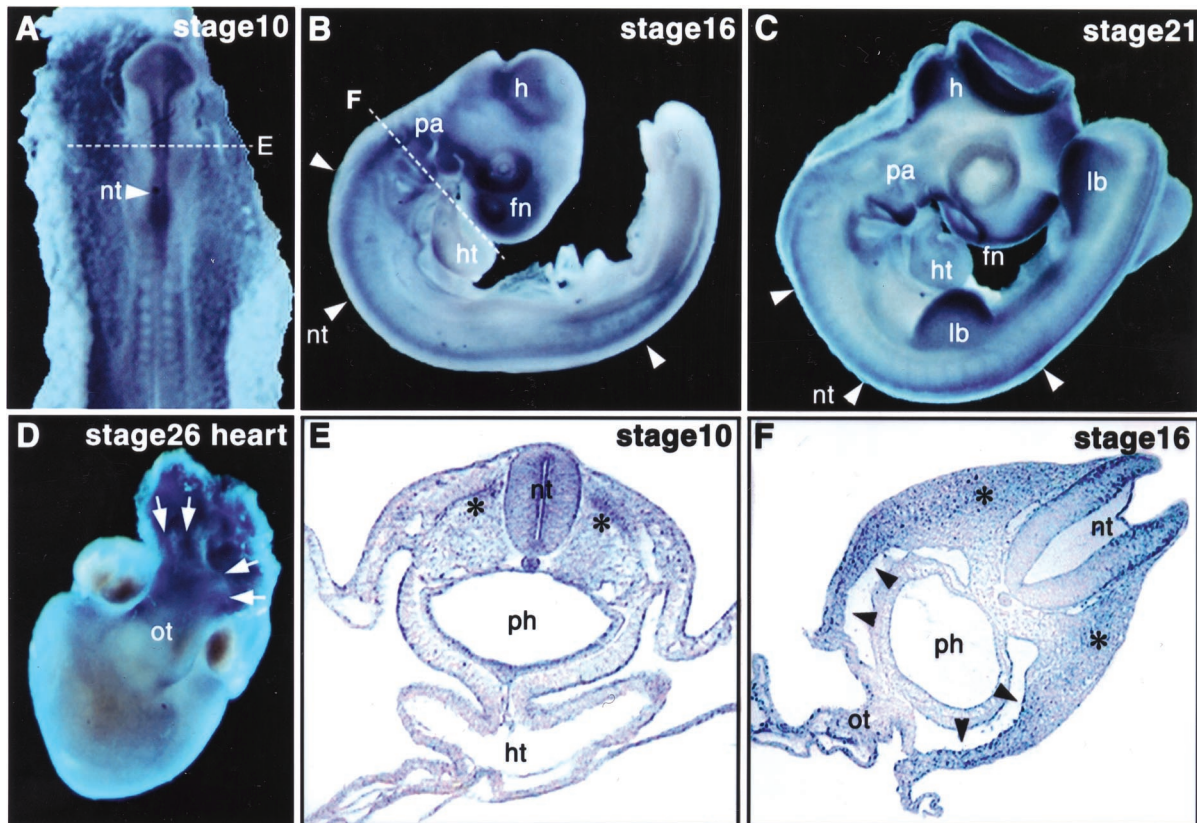

Figure 2. Expression of chick Ufd1l during embryogenesis. *In situ* hybridization of chick *Ufd1l* on stage 10, 16, or 21 chick embryos (*A–C*) and on heart of stage 26 embryo (*D*). At stage 10, the expression throughout the neural tube (nt) was apparent (*A*). At later stages, chick Ufd1l expression was enhanced in the head (h), pharyngeal arches (pa), frontonasal region (fn), neural tube (nt, *white arrow heads*), and limb buds (lb) (*B* and *C*). *D*, Strong expression of chick Ufd1l in the outflow tract (ot) of the heart and arch arteries (*white arrows*). Transverse section of embryo in *A* and *B* after whole-mount *in situ* hybridization (*E* and *F*, respectively) is shown at levels indicated. The expression was observed in the neural tube (nt), cranial mesenchyme (*), aortic arch arteries (*black arrow heads*), and outflow tract (ot) (*E* and *F*). ph, pharynx; ht, heart.
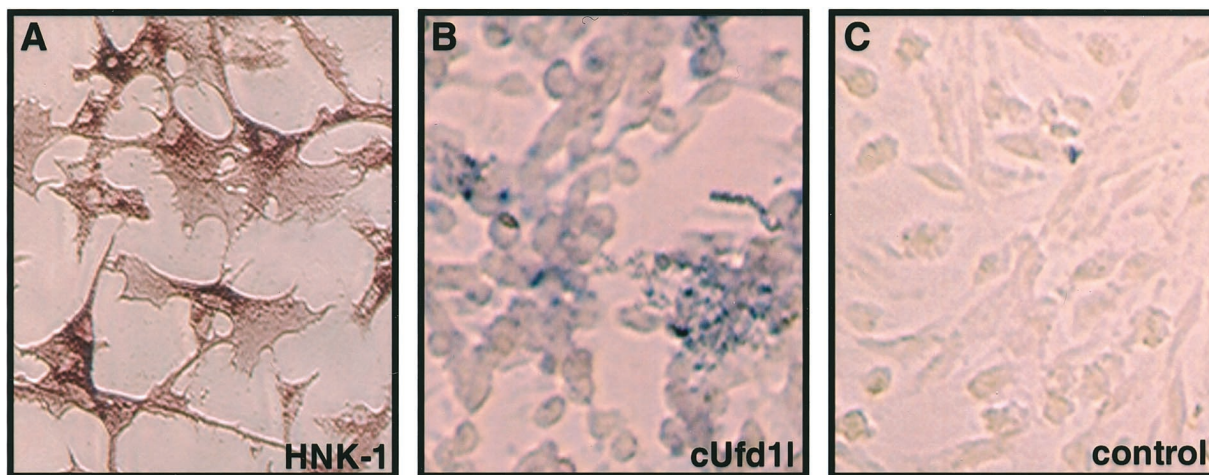
Figure 3. Chick *Ufd1l* is expressed in primary neural crest culture. *A*, HNK-1, as a NCC marker, was detected by immunocytochemistry in primary neural crest cultured cells. *B*, Chick Ufd1l transcripts were detected by antisense mRNA *in situ* hybridization in primary cultured cells. *C*, *In situ* hybridization with sense Ufd1l riboprobe as control.
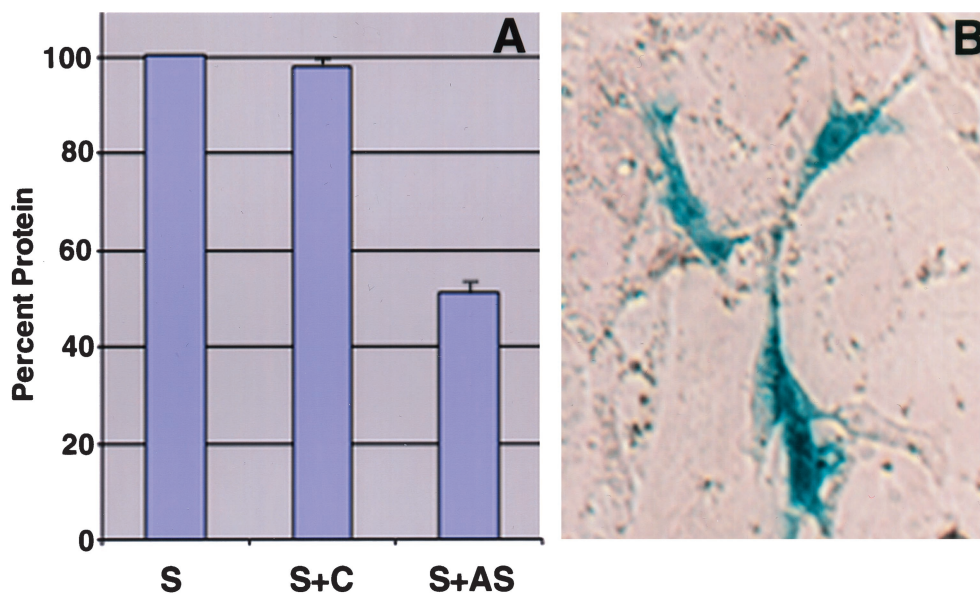

Figure 4. Antisense chick Ufd1l transcripts can attenuate chick Ufd1l protein expression. *A*, Quantitative analysis of *in vitro* transcription and translation reveals a 54% reduction in Ufd1l protein when Ufd1l sense (S) and antisense (AS) transcripts were co-incubated compared with S alone or S with a control (C) antisense (ET_A). The expression of ET_A antisense transcripts did not affect protein expression of chick Ufd1l. *B*, Primary NCC culture after neural tube infection with retrovirus containing the AS Ufd1l expression construct linked to β-galactosidase. Survival and migration of infected cells (blue) were unaffected.

expression of chick Ufd1l was reduced ~50% by expression of the antisense chick Ufd1l transcript. The expression of control (ET_A) antisense transcripts did not affect the protein expression of chick Ufd1l, suggesting that the effect of antisense chick Ufd1l introduction was specific for the reduction of chick Ufd1l protein expression. To determine whether cells infected with the Ufd1l antisense vector had a nonspecific survival defect, we performed primary neural crest culture from neural tube infected with the Ufd1l antisense retrovirus. Retrovirus-infected cells were marked in blue by β-galactosidase staining, and we found that their survival was unaffected by Ufd1l antisense transcripts (Fig. 4B).

For determining the functional role played by chick Ufd1l in cardiac NCC, the rostral neural tube was infected with retrovirus containing the antisense Ufd1l expression construct be-fore NCC migration. By examining the hearts of a number of embryos at HH stage 31–32, 6 d after the retroviral infection, we found a significant ($p < 0.05$) increase in septal defects (nine of 12) compared with control embryos (two of 12 and zero of 12, respectively) that were infected with retrovirus containing an empty vector (Fig. 5, A–F). Five of 12 experimental embryos had defects of the upper portion of the ventricular septum (VSD; Fig. 5, B and E). An additional four of 12 embryos had VSD and defects in septation of the aorta and pulmonary artery (conotruncal septal defects; Fig. 5, C and F). This combination was never observed in control embryos ($p < 0.05$), whereas isolated VSD were observed in two of 12 control embryos. Examination of the aortic arch in all embryos failed to detect any defects at this stage. Results are summarized in Table 1.
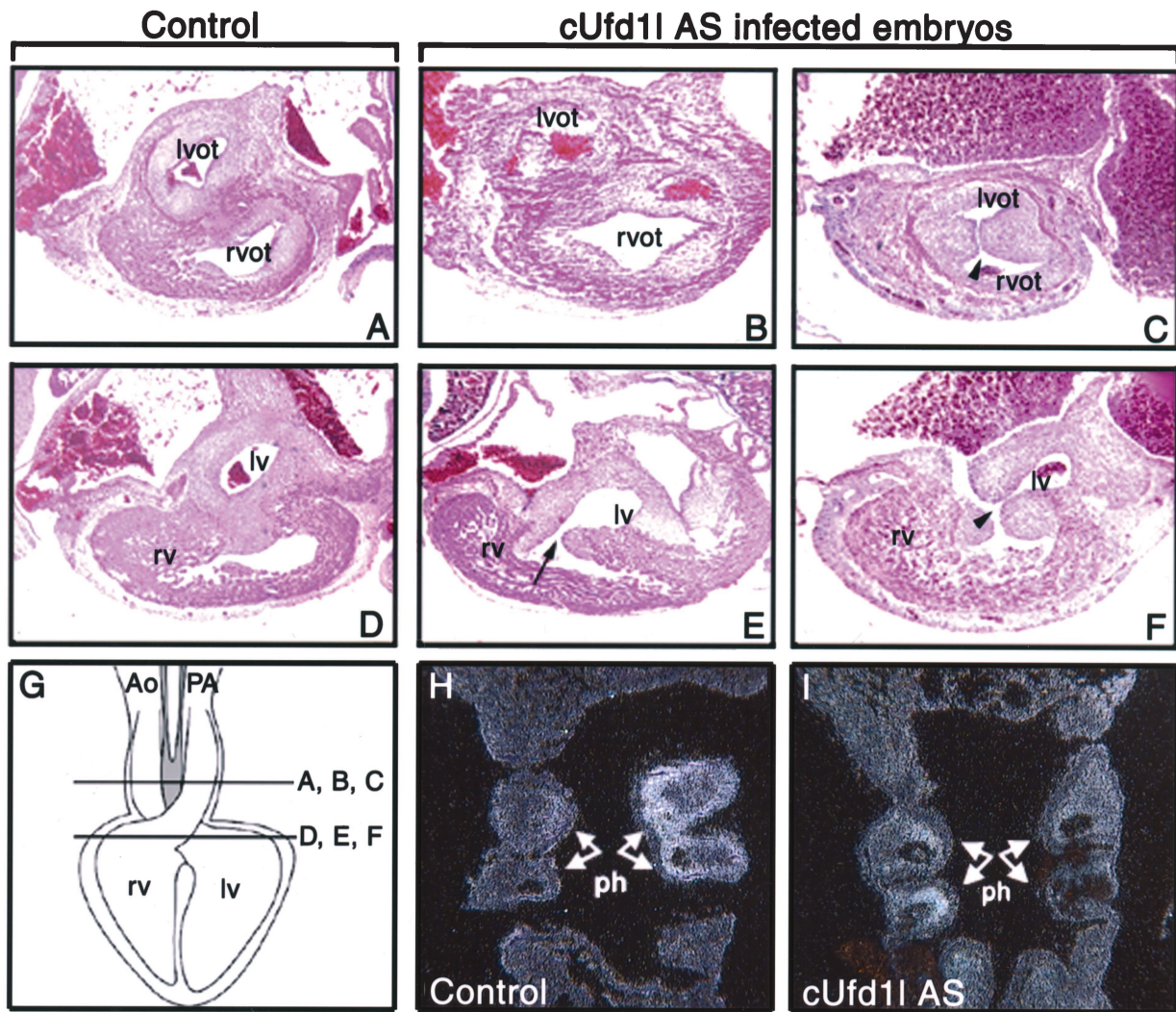
Figure 5. Attenuation of Ufd1l in chick neural crest results in conotruncal defects. Transverse sections of the stage 31–32 chick hearts at the level of the conotruncal septum (*A–C*) or ventricular septum (*D–F*) in control embryos (*A* and *D*) or retrovirus Ufd1l antisense (AS) infected embryos (*B, C, E,* and *F*). *G,* Schematic indicating level of section. Ventricular septal defects (*arrow*) were observed in AS-infected embryos (*B* and *E*). Conotruncal septal defects (*arrowhead* in *C*) accompanied with VSD (*arrowhead* in *F*) were observed in AS-infected embryos. Radioactive RNA *in situ* hybridization on coronal sections of HH stage 18 embryos revealed similar expression of dHAND, a marker of neural crest–derived mesenchyme, in control (*H*) and AS-infected (*I*) embryos. Ao, aorta; PA, pulmonary artery; lv, left ventricle; lvot, left ventricular outflow tract; rv, right ventricle; rvot, right ventricular outflow tract; ph, pharyngeal arch.

Table 1. *cUfd1l AS retrovirus-infected embryos display cardiac outflow tract defects*

	cUfd11 AS	Control vector
Septal defects	75% (9/12)*	17% (2/12)
Conotruncal	33% (4/12)*	0% (0/12)
Ventricular	42% (5/12)	17% (2/12)
Aortic arch defects	0% (0/12)	0% (0/12)
No defects	25% (3/12)*	83% (10/12)

Percentage of affected embryos are indicated; absolute number of affected/total embryos are also shown.

* $p < 0.05$.

To investigate whether NCC were specified and migrated in antisense Ufd1-infected embryos, we examined two molecular markers, dHAND and neuropilin-1, both expressed in the NCC-derived mesenchyme of pharyngeal arches. Expression of dHAND (Fig. 5, H and I) and neuropilin-1 (data not shown) was relatively normal in the pharyngeal arches of HH stage 18 experimental embryos compared with controls. This result suggests that NCC become specified, migrate, and differentiate into mesenchymal cells during early pharyngeal development of antisense Ufd1l-infected embryos. Taken together, these data indicate that functional attenuation of Ufd1l in cardiac NCC leads to an increased incidence of conotruncal septal defects in chick embryos and these defects do not result from nonspecific cell death before NCC migration.

DISCUSSION

Cross-species analysis is sometimes useful in understanding potential causes of human disease. Mice homozygous for deletion of *Ufd1l* are early embryonic lethal, whereas mice heterozygous for a *Ufd1l* mutation are normal, precluding an examination of whether Ufd1l plays a role in cardiac NCC development (16). Antisense nucleotides designed to hybridize to specific mRNA sequences have been used to attenuate the

function of numerous genes both *in vitro* and *in vivo*, including developmentally regulated genes in chick embryos (22–24). By using a replication-incompetent retrovirus that has proved beneficial in studying the avian NCC lineage, we were able to introduce antisense *Ufd1l* transcripts into chick cardiac NCC over long time spans and examine the role of Ufd1l in cardiac NCC *in vivo*.

Although functional attenuation of Ufd1l in NCC lineage resulted in an increased number of conotruncal septal defects in chick embryos, there was phenotypic variation. It is possible that the phenotypic variation may reflect the gene dosage effect of Ufd1l resulting from a variable efficiency of retroviral infection in each chick embryo. If this is the case, then conotruncal septation requires Ufd1l in a dose-sensitive manner in this chick model, although haploinsufficiency of *Ufd1l* alone is not sufficient for the septal defects in the mouse model. Alternatively, it may reflect allelic variability, variable penetrance caused by environmental factors, or stochastic events during embryonic development similar to that proposed in patients with 22q11DS. We cannot distinguish between these possibilities as it is not possible to examine effectively the level of attenuation of Ufd1l protein in premigratory NCC of embryos studied later in development for defects in cardiogenesis.

Recent genomic manipulations in mice have provided insight into potential roles of candidate genes for 22q11DS. Mice harboring a hemizygous deletion of 18 genes, including *Ufd1l*, that are deleted in patients with 22q11DS (*Df1/+*) were generated and exhibit aortic arch malformations in ~30% of cases (16). Further analyses determined that haploinsufficiency of *Tbx1* was responsible for aortic arch malformations in *Df1/+* mice (10). Mice homozygous for the *Tbx1* mutation displayed craniofacial and cardiovascular defects similar to 22q11DS (9–11), suggesting that *TBX1* may be a major determinant of the phenotype of 22q11DS. However, *TBX1* mutations have not been identified in patients who have the 22q11 deletion phenotype and do not have del.22q11 (10, 13). In addition, *Df1/+* mice have broader phenotypic features that have not been observed in mice heterozygous for a *Tbx1* mutation, including conotruncal and ventricular septal defect, hypoplasia of thymus and parathyroid glands, and signs of behavioral and psychiatric disorder (16, 25, 26). These results indicate that haploinsufficiency of *Tbx1* and additional genes in the *Df1* deletion region together contribute to the entire phenotype of *Df1/+* mice. Our data in the present study suggest a role for Ufd1l in conotruncal development and thus support a possibility that *Ufd1l* may contribute to conotruncal and ventricular septal defects as a modifier gene in *Df1/+* mice. *Ufd1l* might also contribute to the hypoplasia of the thymus/parathyroid glands and behavioral/psychiatric phenotype of *Df1/+* mice, because it is expressed in the developing pharyngeal structures and brain. The association of a promoter polymorphism of UFD1L with schizophrenia susceptibility has recently been reported (27). Definitive evaluation of Ufd1l's role in particular tissues awaits tissue-specific disruption of *Ufd1l* in mice, currently being performed in our laboratory.

Although we determined that Ufd1l plays a role in cardiac NCC, cellular functions of Ufd1l in avian or mammalian cells remain to be studied. We speculate that Ufd1l is required for postmigratory differentiation of cardiac NCC in the conotruncal region because *1*) the infection of retrovirus containing antisense *Ufd1l* did not affect NCC survival and migration in primary NCC; *2*) Ufd1l was expressed at high levels in the conotruncal region; and *3*) functional attenuation of Ufd1l resulted in conotruncal septation defects, although the phenotype was milder than that observed after ablation of premigratory NCC in chick embryos. Recent biochemical studies demonstrated multiple functions of Ufd1, including the activation of membrane-bound transcription factors and transportation of proteins from the endoplasmic reticulum into the cytosol, by regulating ubiquitin/proteosome-dependent processing (28–31). Identification of pathways affected by Ufd1l in cardiac NCC will be necessary to understand the mechanism through which Ufd1l regulates NCC development.

REFERENCES

1. Scambler PJ 2000 The 22q11 deletion syndromes. Hum Mol Genet 9:2421–2426
2. Driscoll DA, Budarf ML, Emanuel BS 1992 A genetic etiology for DiGeorge syndrome: consistent deletions and microdeletions of 22q11. Am J Hum Genet 50:924–933
3. Scambler PJ, Kelly D, Lindsay E, Williamson R, Goldberg R, Shprintzen R, Wilson DI, Goodship JA, Cross IE, Burn J 1992 Velo-cardio-facial syndrome associated with chromosome 22 deletions encompassing the DiGeorge locus. Lancet 339:1138–1139
4. Burn J, Takao A, Wilson D, Cross I, Momma K, Wadey R, Scambler P, Goodship J 1993 Conotruncal anomaly face syndrome is associated with a deletion within chromosome 22q11. J Med Genet 30:822–824
5. Ryan AK, Goodship JA, Wilson DI, Philip N, Levy A, Seidel H, Schuffenhauer S, Oechsler H, Belohradsky B, Prieur M, Aurias A, Raymond FL, Clayton-Smith J, Hatchwell E, McKeown C, Beemer FA, Dallapiccola B, Novelli G, Hurst JA, Ignatius J, Green AJ, Winter RM, Brueton L, Brondum-Nielsen K, Stewart F, Essen TV, Patton M, Paterson J, Scambler PJ 1997 Spectrum of clinical features associated with interstitial chromosome 22q11 deletions: a European collaborative study. J Med Genet 34:798–804
6. Kirby ML, Gale TF, Stewart DE 1983 Neural crest cells contribute to normal aorticopulmonary septation. Science 220:1059–1061
7. Kirby ML, Waldo KL 1995 Neural crest and cardiovascular patterning. Circ Res 77:211–215
8. Lindsay EA 2001 Chromosome microdeletions Dissecting del22q11 syndrome. Nat Rev Genet 2:858–868
9. Merscher S, Funke B, Epstein JA, Heyer J, Puech A, Lu MM, Xavier RJ, Demay MB, Russell RG, Factor S, Tokooya K, Jore BS, Lopez M, Pandita RK, Lia M, Carrion D, Xu H, Schorle H, Kobler JB, Scambler P, Wynshaw-Boris A, Skoultchi AI, Morrow BE, Kucherlapati R 2001 TBX1 is responsible for cardiovascular defects in velo-cardio-facial/DiGeorge syndrome. Cell 104:619–629
10. Lindsay EA, Vitelli F, Su H, Morishima M, Huynh T, Pramparo T, Jurecic V, Ogunrinu G, Sutherland HF, Scambler PJ, Bradley A, Baldini A 2001 Tbx1 haploinsufficiency in the Di George syndrome region causes aortic arch defects in mice. Nature 410:97–101
11. Jerome LA, Papaioannou VE 2001 Di George syndrome phenotype in mice mutant for the T-box gene, Tbx1. Nat Genet 27:286–291
12. Wadey R, McKie J, Papapetrou C, Sutherland H, Lohman F, Osinga J, Frohn I, Hofstra R, Meijers C, Amati F, Conti E, Pizzuti A, Dallapiccola B, Novelli G, Scambler P 1999 Mutations of UFD1L are not responsible for the majority of cases of DiGeorge Syndrome/velocardiofacial syndrome without deletions within chromosome 22q11. Am J Hum Genet 65:247–249
13. Gong W, Gottlieb S, Collins J, Blescia A, Dietz H, Goldmuntz E, McDonald-McGinn DM, Zackai EH, Emanuel BS, Driscoll DA, Budarf ML 2001 Mutation analysis of TBX1 in non-deleted patients with features of DGS/VCFS or isolated cardiovascular defects. J Med Genet 38:E45
14. Pizzuti A, Novelli G, Ratti A, Amati F, Mari A, Calabrese G, Nicolis S, Silani V, Marino B, Scarlato G, Ottolenghi S, Dallapiccola B 1997 UFD1L, a developmentally expressed ubiquitination gene, is deleted in CATCH 22 syndrome. Hum Mol Genet 6:259–265
15. Yamagishi H, Garg V, Matsuoka R, Thomas T, Srivastava D 1999 A molecular pathway revealing a genetic basis for human cardiac and craniofacial defects. Science 283:1158–1161
16. Lindsay EA, Botta A, Jurecic V, Carattini-Rivera S, Cheah YC, Rosenblatt HM, Bradley A, Baldini A 1999 Congenital heart disease in mice deficient for the DiGeorge syndrome region. Nature 401:379–383

17. Hyer J, Mikawa T 1997 Retroviral techniques for studying organogenesis with a focus on heart development. Mol Cell Biochem 172:23–35
18. Garg V, Yamagishi C, Hu T, Kathiriya IS, Yamagishi H, Srivastava D 2001 Tbx1, a Di George syndrome candidate gene, is regulated by sonic hedgehog during pharyngeal arch development. Dev Biol 235:62–73
19. Bergwerff M, Verberne ME, DeRuiter MC, Poelmann RE, Gittenberger-de Groot AC 1998 Neural crest cell contribution to the developing circulatory system: implications for vascular morphology? Circ Res 82:221–231
20. Poelmann RE, Mikawa T, Gittenberger-de Groot AC 1998 Neural crest cells in outflow tract septation of the embryonic chicken heart: differentiation and apoptosis. Dev Dyn 212:373–84
21. Kunte A, Ivey K, Yamagishi C, Garg V, Yamagishi H, Srivastava D 2001 A common cis-acting sequence in the DiGeorge critical region regulates bi-directional transcription of UFD1L and CDC45L. Mech Dev 108:81–92
22. Farrell MJ, Stadt H, Wallis KT, Scambler P, Hixon RL, Wolfe R, Leatherbury L, Kirby ML 1999 HIRA, a DiGeorge syndrome candidate gene, is required for cardiac outflow tract septation. Circ Res 84:127–135
23. Isaac A, Sargent MG, Cooke J 1997 Control of vertebrate left-right asymmetry by a Snail-related zinc finger gene Science 275:1301–1304
24. Lallier T, Bronner-Fraser M 1993 Inhibition of neural crest cell attachment by integrin antisense oligonucleotides. Science 259:692–695
25. Taddei I, Morishima M, Huynh T, Lindsay EA 2001 Genetic factors are major determinants of phenotypic variability in a mouse model of the DiGeorge/del 22q11 syndromes. Proc Natl Acad Sci U S A 98:11428–11431
26. Paylor R, McIlwain KL, McAninch R, Nellis A, Yuva-Paylor LA, Baldini A, Lindsay EA 2001 Mice deleted for the DiGeorge/velocardiofacial syndrome region show abnormal sensorimotor gating and learning and memory impairments. Hum Mol Genet 10:2645–2650
27. De Luca A, Pasini A, Amati F, Botta A, Spalletta G, Alimenti S, Caccamo F, Conti E, Trakalo J, Macciardi F, Dallapiccola B, Novelli G 2001 Association study of a promoter polymorphism of UFD1L gene with schizophrenia. Am J Med Genet 105:529–533
28. Meyer HH, Shorter JG, Seemann J, Pappin D, Warren G 2000 A complex of mammalian ufd1 and npl4 links the AAA-ATPase, p97, to ubiquitin and nuclear transport pathways. EMBO J 19:2181–2192
29. Hoppe T, Matuschewski K, Rape M, Schlenker S, Ulrich HD, Jentsch S 2000 Activation of a membrane-bound transcription factor by regulated ubiquitin/proteosome-dependent processing. Cell 102:577–586
30. Rape M, Hoppe T, Gorr I, Kalocay M, Richly H, Jentsch S 2001 Mobilization of processed, membrane-tethered SPT23 transcription factor by CDC48 (UFD1/NPL4), a ubiquitin-selective chaperone. Cell 107:667–677
31. Ye Y, Meyer HH, Rapoport TA 2001 The AAA ATPase Cdc48/p97 and its partners transport proteins from the ER into the cytosol. Nature 414:652–656